ACCOUNTS of chemical research

Article

pubs.acs.org/accounts

Energy Cascades, Excited State Dynamics, and Photochemistry in Cob(III)alamins and Ferric Porphyrins

Published as part of the Accounts of Chemical Research special issue "Ultrafast Excited-State Processes in Inorganic Systems".

Aaron S. Rury, Theodore E. Wiley, and Roseanne J. Sension*

Department of Chemistry and Department of Physics, University of Michigan, Ann Arbor, Michigan 48109-1055, United States

CONSPECTUS: Porphyrins and the related chlorins and corrins contain a cyclic tetrapyrrole with the ability to coordinate an active metal center and to perform a variety of functions exploiting the oxidation state, reactivity, and axial ligation of the metal center. These compounds are used in optically activated applications ranging from light harvesting and energy conversion to medical therapeutics and photodynamic therapy to molecular electronics, spintronics, optoelectronic thin films, and optomagnetics. Cobalt containing corrin rings extend the range of applications through photolytic cleavage of a unique axial carbon−cobalt bond, permitting spatiotemporal control of drug delivery.

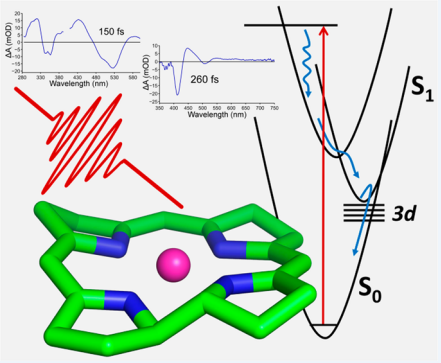

The photochemistry and photophysics of cyclic tetrapyrroles are controlled by electronic relaxation dynamics including internal conversion and intersystem crossing. Typically the electronic excitation cascades through ring centered $\pi\pi^*$ states, ligand to metal charge transfer (LMCT) states, metal to ligand charge transfer (MLCT) states, and metal centered states. Ultrafast transient absorption spectroscopy provides a powerful tool for the investigation of the electronic state dynamics in metal containing tetrapyrroles. The UV−visible spectrum is sensitive to the oxidation state, electronic configuration, spin state, and axial ligation of the central metal atom. Ultrashort broadband white light probes spanning the range from 270 to 800 nm, combined with tunable excitation pulses, permit the detailed unravelling of the time scales involved in the electronic energy cascade. State-of-the-art theoretical calculations provide additional insight required for precise assignment of the states.

In this Account, we focus on recent ultrafast transient absorption studies of ferric porphyrins and corrin containing cob(III)alamins elucidating the electronic states responsible for ultrafast energy cascades, excited state dynamics, and the resulting photoreactivity or photostability of these compounds. Iron tetraphenyl porphyrin chloride ($Fe^{(III)}$TPPCl) exhibits picosecond decay to a metal centered d → d* ^{4}T state. This state decays on a ca. 16 ps time scale in room temperature solution but persists for much longer in a cryogenic glass. The photoreactivity of the ^{4}T state may lead to novel future applications for these compounds. In contrast, the nonplanar cob(III)alamins contain two axial ligands to the central cobalt atom. The upper axial ligand can be an alkyl group as in the two biologically active coenzymes or a nonalkyl ligand such as −CN in cyanocobalamin (vitamin B_{12}) or −OH in hydroxocobalamin. The electronic structure, energy cascade, and bond cleavage of these compounds is sensitive to the details of the axial ligand. Nonalkylcobalamins exhibit ultrafast internal conversion to a low-lying state of metal to ligand or ligand to metal charge transfer character. The compounds are generally photostable with ground state recovery complete on a time scale of 2−7 ps in room temperature aqueous solution. Alkylcobalamins exhibit ultrafast internal conversion to an S_1 state of $d/\pi \rightarrow \pi^*$ character. Most compounds undergo bond cleavage from this state with near unit quantum yield within ∼100 ps. Recent theoretical calculations provide a potential energy surface accounting for these observations. Conformation dependent mixing of the corrin π and cobalt d orbitals plays a significant role in the observed photochemistry and photophysics.

1. INTRODUCTION

Porphyrins and related chlorins and corrins (Figure 1) comprise a family of critical cofactors utilized in a wide range of natural and synthetic materials. These cyclic tetrapyrroles have the ability to coordinate a range of active metal atoms and to perform a variety of different functions that exploit the oxidation state, electronic structure, and axial ligation of the metal center. Many key applications involve ground state chemistry of the metal center. However, the conjugated tetrapyrrole rings are strongly absorbing chromophores with electronic transitions in the visible and ultraviolet regions of the spectrum. This strong optical absorption leads to a range of photoactivated applications. The most obvious example is the role that chlorophyll and bacteriochlorophyll play in photosynthesis.[1] However, potential applications extend far beyond light-harvesting.

Received: November 1, 2014
Published: March 5, 2015

DOI: 10.1021/ar5004016
Acc. Chem. Res. 2015, 48, 860−867

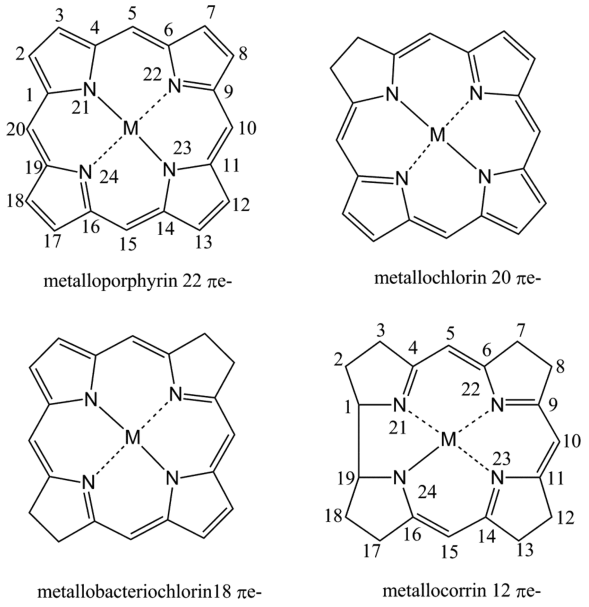

Figure 1. Schematic diagram of metal containing cyclic tetrapyrroles.

Natural and synthetic metalloporphyrins are used in energy conversion, medical therapeutics, photodynamic therapy, molecular electronics, spintronics, optoelectronic thin films, and optomagnetics.[2−7] Most of these applications involve electron dynamics, including population of electronically excited states and charge separation from a donor to an acceptor. However, some applications exploit the axial ligation of the central metal atom. The number of axial ligands is determined by the electronic configuration, oxidation state, and spin state of the central metal. These ligands can be bound, transported, and following optical excitation, transformed or released.

The interest in metallocorrins as photoactivated agents has developed somewhat slower than porphyrins, but applications are now appearing. Cobalamin is a cobalt−corrin compound incorporated as an alkyl derivative into a variety of enzymes including two human enzymes.[8,9] Alkylcobalamins possess a unique carbon−cobalt bond capable of thermal and photolytic cleavage producing a range of reactive organic ions and radicals.[10−14] Potential applications of cobalamins include spatiotemporal control of drug delivery through C−Co bond cleavage[15,16] and optically controlled formation of OH radicals throuch O−Co bond cleavage.[17] These applications complement the range of applications proposed for metalloporphyrins.

The photochemistry and photophysics of cyclic metallotetrapyrroles are controlled by electronic relaxation dynamics including internal conversion and intersystem crossing. Typically the electronic excitation cascades through ring centered $\pi\pi^*$ states, ligand to metal charge transfer (LMCT) states, metal to ligand charge transfer (MLCT) states, and metal centered states. Often these dynamics are ultrafast, occurring on sub-picosecond and picosecond time scales.[5,18−21] A detailed understanding of these processes requires both careful experimental work and state-of-the-art theoretical calculation. Ultrafast transient absorption spectroscopy has proven to be a powerful technique for the investigation of these dynamics. In this Account, we will focus on recent ultrafast transient absorption studies of cob(III)-alamins and ferric porphyrins elucidating the electronic states responsible for ultrafast energy cascades, excited state dynamics, and the resulting photoreactivity or photostability of these compounds.

Theoretical calculations necessary to interpret and predict the photochemistry and photophysics of porphyrins and cobalamins are complicated by the size of the tetrapyrrole ring, the presence of a variety of pendant groups, the complexity of the metal center, and the importance of charge transfer states. Nonetheless, significant progress has been made and theoretical methods are being developed to calculate the electronic state potential energy surfaces of a variety of systems away from the vertical Franck−Condon region. These calculations provide insight into the energy cascade in metal containing corrins, porphyrins, and other cyclic tetrapyrroles.[22−33] The experimental results will be discussed in the context of these recent calculations.

2. FERRIC PORPHYRINS

The oxidation state of the Fe atom ligated to a porphyrin ring plays an important role in the reactivity and dynamics of iron porphyrins. In its ferric form, the oxidation state of iron is +3. In the porphyrin structure, this oxidation state allows for ligation of the four ring-bound nitrogen atoms and one or two axial ligands. The five 3d electrons of iron provide the possibility of $S = 5/2$, $S = 3/2$, and $S = 1/2$ spin states depending on the occupation of the t_{2g} and e_g atomic states. The ligand field splitting of these states largely determines the spin configuration of the Fe.

Two dominant features stand out in the UV−visible (UV−vis) spectra of ferric porphyrins (Figure 2), a strong peak near

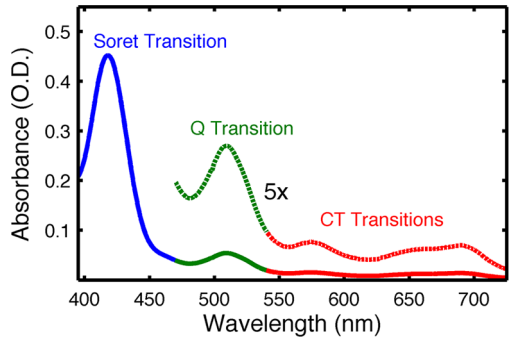

Figure 2. Room temperature UV−vis absorption spectrum of $Fe^{(III)}$TPPCl dissolved in a 1:1 mixture of toluene and CH_2Cl_2 highlighting the dominant Soret (blue) and Q transitions (green) as well as the weaker, lower frequency CT transitions (red) of ferric porphyrins.

400 nm, associated with the singlet−singlet $S_0 \rightarrow S_2$ transition of the porphyrin macrocycle often denoted the Soret resonance, and a second set of features at longer wavelengths associated with the lowest energy singlet transition, $S_0 \rightarrow S_1$ of the porphyrin ring, known as the Q resonances. Other transitions, including charge transfer states between the Fe atom and its ligands, typically appear outside of these spectral windows.

Over the past decade, it had become generally accepted that electronic relaxation of iron hemes, especially ferric hemes, is ultrafast with internal conversion to the ground state occurring on a sub-picosecond time scale.[34] The same was expected to hold for other ferric porphyrins. Recent careful transient absorption studies have demonstrated that this is not true in general.[18,19,35] A careful study of Met-myoglobin points to a branched pathway with a cascade through spin states on a picosecond time scale.[18] In another study, discussed in more detail here, the formation of long-lived iron spin states has important consequences for the photostability of iron tetraphenylporphyrin.[35]

DOI: 10.1021/ar5004016
Acc. Chem. Res. 2015, 48, 860−867

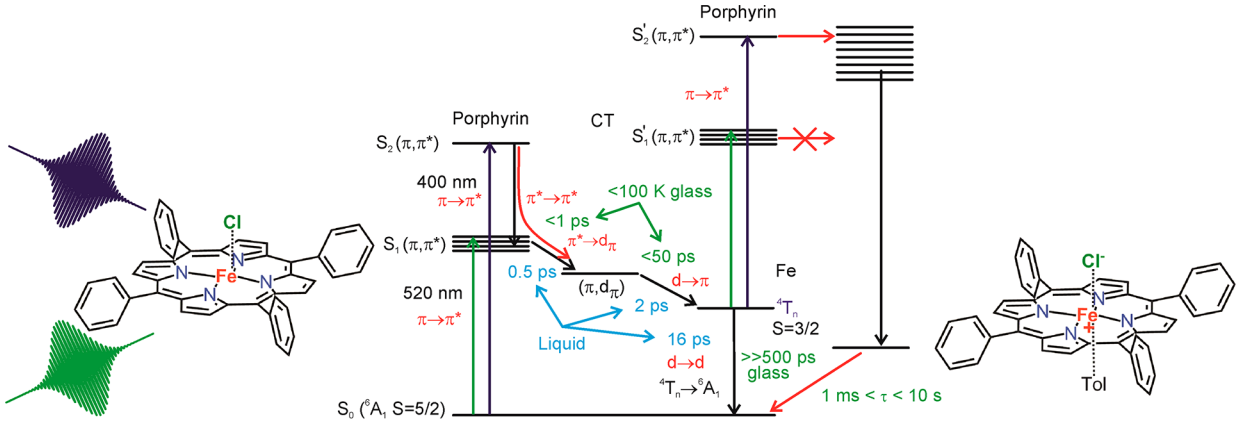

Figure 3. Schematic summary of the photochemistry and photophysics observed for $Fe^{(III)}$TPPCl in a 1:1 mixture of toluene and CH_2Cl_2 as a room temperature liquid and a cryogenic glass.

2.1. Excited State Dynamics of $Fe^{(III)}$TPPCl

Given the interest in a wide variety of Fe-bound porphyrins, model systems providing general principles of excited state dynamics and reactivity become useful. One such model system is iron(III) tetraphenylporphyrin chloride [$Fe^{(III)}$TPPCl]. In this complex, the central iron atom is in a five-coordinate high spin $S = 5/2$ state, binding a chloride ion in the axial position. This compound has been characterized using a variety of spectroscopic techniques and theoretical calculations.[36,37]

Ultrafast broadband transient absorption spectroscopy of $Fe^{(III)}$TPPCl in solution was used to study the excited state relaxation for excitation in the Soret (400 nm) and Q-band (520 nm) resonances.[19] Figure 3 summarizes the results. Following excitation at 400 nm, there is a ~0.1 ps component associated with the internal conversion of the initially prepared S_2 state to the excited S_1 manifold. This physical interpretation is consistent with a weak but measurable steady-state fluorescence signal observed in a spectral region qualitatively agreeing with emission from an $S_2 \rightarrow S_0$ transition. Subsequent dynamics are the same for both excitation wavelengths. The spectral characteristics of the next two excited states populated, with lifetimes of ~0.5 and 2 ps, respectively, are consistent with the singlet electronic states of metalloporphyrins as described previously.[38,39]

The spectrum of the longest-lived excited state is consistent with population of an excited atomic state of the central iron atom. This state forms through sequential LMCT and MLCT processes to produce a porphyrin macrocycle in its ground state and the excited d−d* atomic state, either the $^4T_1$ or $^4T_2$ state.[19,36,37]

For temperatures below 100 K in a 1:1 toluene and CH_2Cl_2 glass, the first three relaxation processes following excitation of ground state $Fe^{(III)}$TPPCl remain ultrafast with the charge transfer (π,d_π) state formed within a picosecond and the subsequent decay to the ^4T_n state complete within 50 ps.[35] However, the lifetime of the ^4T_n state increases by at least a factor of 50 with minimal depletion of the population between 50 to 500 ps, implying an energy barrier preventing ground state recovery at low temperature.[35]

2.2. Photochemical Reactivity of $Fe^{(III)}$TPPCl

In addition to the significant increase in the lifetime of the excited ^4T_n state localized on the iron atom, new spectroscopic signatures appear in the difference spectra of $Fe^{(III)}$TPPCl in TA measurements at sub-100 K temperatures. A long-lived product (>1 ms) results in a large amplitude difference spectrum that is qualitatively different from the ground state spectrum of $Fe^{(III)}$TPPCl.

The long-lived product was characterized using steady-state resonance Raman spectroscopy.[35] Resonance Raman (rR) spectroscopy has also proven to be a useful tool in characterizing the connection of electronic and nuclear structure with the oxidation and spin states of the ferric porphyrins.[40] In particular, several studies catalogue the position and relative magnitude of a series of structure-sensitive Raman modes of the porphyrin macrocycle as a function of metal oxidation state, spin state, and ligation.[41−43] Therefore, one can use the position of one or more of these modes in the rR spectrum to determine characteristics such as the oxidation and spin state of a central metal atom in an unknown metalloporphyrin.

The steady-state rR spectrum of $Fe^{(III)}$TPPCl in a 1:1 glass of CH_2Cl_2 and toluene at 77 K obtained with 413 nm continuous-wave excitation exhibits a power dependence in the region containing several structure-sensitive interior porphyrin ring vibrations (1100−1700 cm^{-1}) (Figure 4). This power dependence is

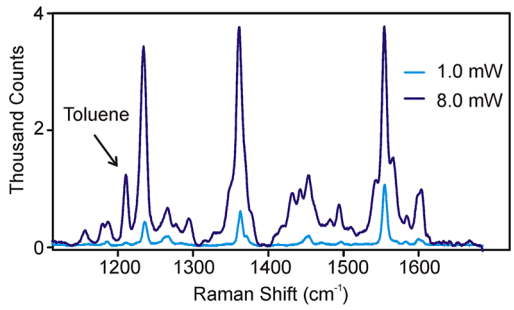

Figure 4. Resonance Raman spectra of Fe(III)TPPCl as a function of incident laser power at 413 nm. The key features to note are the toluene band at 1210 cm^{-1} and the triplets in the regions around 1550, 1440, and 1360 cm^{-1}.

an indication that $Fe^{(III)}$TPPCl undergoes photochemical changes when excited on its Soret resonance at low temperature. The new peaks following excitation at 413 nm represent the formation of new FeTPP species following two-photon excitation as illustrated in Figure 3. In contrast, we observe no power dependent changes in the rR spectra of $Fe^{(III)}$TPPCl in the same 77 K glass when exciting in the Q-band at either 488 or 514 nm.

The rR spectrum is used to characterize the nature of the long-lived photoproduct. Most conspicuous, triplets of peaks appear

DOI: 10.1021/ar5004016
Acc. Chem. Res. 2015, 48, 860−867

in the regions of the ν_2 (~1550 cm^{-1}), ν_3 (~1440 cm^{-1}), and ν_4 (~1360 cm^{-1}) A_{1g} totally symmetric vibrations of the porphyrin macrocycle. The exact position of these vibrations is sensitive to the oxidation and spin states of the metal.[41−43] The observed triplets of peaks are consistent with the formation of three products possessing centrally ligated Fe atoms in three distinct states: a five-coordinate high-spin state, a six-coordinate high-spin state, and a six-coordinate low-spin state. In addition, two new power dependent peaks in the rR spectra indicate a resonant enhancement of toluene Raman modes. This signifies coordination of toluene in the six-coordinate high- and low-spin products, as observed in the crystalline phase.[44,45] The low-spin state likely forms due to an increased ligand field splitting of the t_{2g} and e_g d-electronic states of the Fe atom following toluene ligation.

With both the temperature dependent ultrafast TA and power dependent rR measurements, a more complete picture of this photochemical process emerges (Figure 3). First, absorption of a 413 nm photon leads to the formation of an excited FeTPPCl with a lifetime on the order of a nanosecond where the Fe atom is in a d−d* ^4T_n state. Second, the porphyrin ring of the excited FeTPPCl absorbs an additional 413 nm photon, producing a $\pi-\pi^*$ S_2' state with multiple relaxation pathways that compete effectively with internal conversion to the S_1' state. Given that the S_2' state is accessible via Soret excitation but not Q resonance excitation, this must be the state controlling the observed photochemistry. Along at least two of these relaxation paths, an atomic Fe state is produced such that toluene becomes bound to the complex and causes a change in the spin state of the atom for a substantial portion of the ensemble of excited complexes. The localized d orbitals of Fe play a key role in these processes

3. COBALAMINS

Cobalamins provide an interesting contrast to FeTPPCl. Again the internal conversion dynamics involve a cascade through states involving both π orbitals of the tetrapyrrole and d orbitals of the central metal atom. However, the corrin ring is not planar, and as a consequence the states of the system involve more extensive mixing of contributions from the π orbitals of the corrin and the d orbitals of the cobalt. This influences electronic configurations, the potential energy surfaces, and the excited state dynamics.

The most common oxidation state for stable cobalamin species is the Co^{3+} or cob(III)alamin state. In this oxidation state, there are generally two axial ligands to the cobalt atom (Figure 5). The upper axial ligand can be an alkyl group as in the two biologically active coenzymes methylcobalamin (MeCbl) and 5′-deoxyadenosyl (coenzyme B_{12}, AdoCbl) or a non-alkyl ligand such as −CN in cyanocobalamin (vitamin B_{12}, CNCbl) or −OH in hydroxocobalamin (OHCbl). In solution, the dimethylbenzamidizole base provides the lower axial ligand. When the cobalamin is bound to a protein, the lower axial ligand can be modified by the environment with a histidine residue or a water molecule ligating the cobalt.[46−48]

The axial ligands of the cobalt atom modify the electronic structure and consequently the photochemistry and photophysics of the cobalamin molecule. The UV−visible absorption spectrum reflects these changes in electronic structure (Figure 6). The position and structure of the $\alpha\beta$ band is characteristic of the axial ligands. Most notably, this band blue shifts when the upper ligand is removed forming cob(II)alamin or when the lower ligand is replaced by water.

The excited state dynamics in a number of alkyl and non-alkyl cobalamins have been examined using ultrafast transient absorption spectroscopy.[11−14,20,21,49] The electronic spectra of

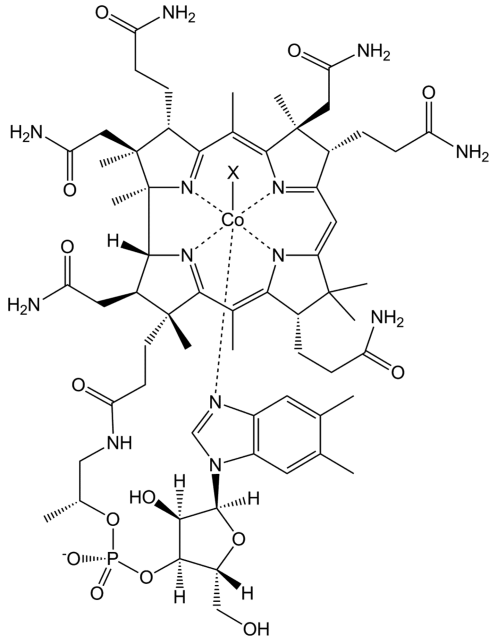

Figure 5. Cobalamin. In typical non-alkyl cobalamins X is −OH, −CN, $-OH_2$, $-N_3$, or another similar species. Biologically active alkylcobalamins have a carbon−cobalt bond with a methyl group or a 5′-deoxyadenosyl group.

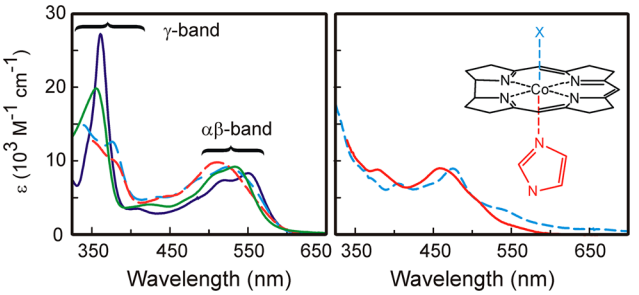

Figure 6. (left) Representative absorption spectra of cob(III)alamins with upper and lower axial ligands. Dashed lines represent n- PrCbl (red) and AdoCbl (lt. blue). Solid lines represent OHCbl (green) and CNCbl (blue). (right) Base-off AdoCbl (red) and cob(II)alamin (light blue dashed).

the low-lying electronic states exhibit spectral shifts similar to those observed for ground state cobalamins. In particular, a blue shift of the $\alpha\beta$ band reflects changes in the axial bonds in the electronic excited states. In what follows, we will compare state-of-the-art TD-DFT quantum chemical calculations,[16,22−26,50−53] with experimental measurements for several cob(III)alamins.

3.1. Non-alkyl Cobalamins

Non-alkyl cobalamins are generally photostable. Electronic excitation leads to a sequence of internal conversion processes repopulating the ground electronic state on a picosecond time scale. Ultrafast transient absorption spectra of CNCbl, H_2OCbl, OHCbl, and N_3Cbl are characterized by nonradiative relaxation within 2−7 ps in room temperature aqueous solution with little or no permanent photoproduct formation.[20,21,49] The electronic states of CNCbl and OHCbl have been calculated using TD-DFT methods allowing comparison between the experimental results and theoretical predictions.[22,24]

3.1.1. Cyanocobalamin. Excitation of CNCbl at 266, 400, or 520 nm populates excited states possessing $\pi \rightarrow \pi^*$ character.

DOI: 10.1021/ar5004016
Acc. Chem. Res. 2015, 48, 860−867

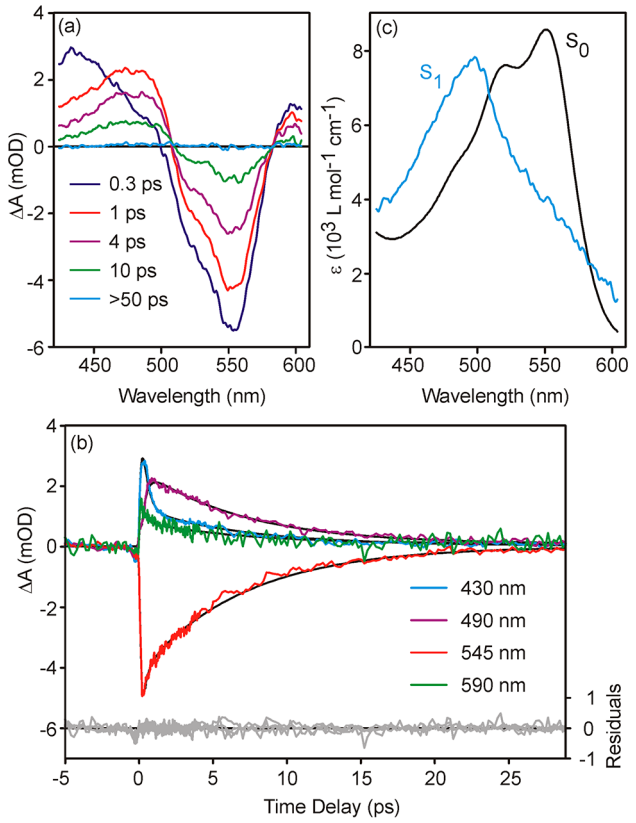

Figure 7. (a) Transient absorption data obtained following 266 nm excitation of CNCbl in water at room temperature, ca. 20 °C. (b) The traces fit well to a 300 fs rise in the S_1 state population, followed by a 6.9 ps decay to baseline. An additional fast component, ≤100 fs, is required on the blue side of the spectrum. (c) Estimated S_1 spectrum compared with S_0.

Typical data obtained with 266 nm excitation are shown in Figure 7. Following excitation at 520 nm, internal conversion from the initially excited state to a lower-lying state occurs on an 80 fs time scale. This is followed by internal conversion to a relaxed S_1 state on a 190 fs time scale.[21] Similar results are obtained with 400 nm excitation, while formation of the S_1 state is slightly slower following 266 nm excitation. The S_1 population subsequently returns to the ground state on a 6.7 ± 0.2 ps time scale in water at room temperature.[21] Slightly longer lifetimes are reported following excitation of CNCbl at 375 nm in D_2O.[49] Significantly longer lifetimes, up to 16 ps, are reported for the S_1 state in less polar solvents.[20,21] The spectral changes observed in the transient IR and UV−visible absorption spectra are consistent with elongation of the axial bonds in the S_1 state.[20,21]

These experimental results agree well with TD-DFT calculations of a CNCbl model compound reported by Kozlowski and co-workers.[22] Their calculations predict that internal conversion from the initially excited $\pi \rightarrow \pi^*$ manifold involves formation of an intermediate $\pi \rightarrow$ d LMCT state followed by geometry relaxation and internal conversion to the S_1 $\pi \rightarrow \sigma^*(d_z^2)$ LMCT state. The minimum energy geometry of the S_1 state is characterized by lengthened axial ligand bonds, with an increase in the Co−C bond from 1.857 to 2.216 Å and an increase in the Co−N_{Im} bond from 2.054 to2.275 Å. The calculated barrier for internal conversion from the S_1 minimum energy configuration is 5.0 kcal/mol in reasonable agreement with the experimental measurement of 2.1 kcal/mol in water at room temperature.[20]

3.1.2. Hydroxocobalamin. Interest in the photochemistry of OHCbl has been stimulated by recent work of Shell and Lawrence where photolysis of OHCbl was used to hydroxylate DNA *in situ*.[17] Their results demonstrate that supercoiled plasmid DNA will relax when it is irradiated with OHCbl in the presence of oxygen. The proposed mechanism involves homolytic cleavage of the Co−O bond to form hydroxyl. Transient absorption measurements have the potential to shed light on this mechanism.

The electronic excited state decay observed following excitation of OHCbl is similar to CNCbl. Excitation of OHCbl in D_2O with 375 pulses results in immediate population of a high lying excited state, which decays on a sub-picosecond timescale (ca. 400 fs) to the S_1 state, followed by a ca. 2.9 ps decay to the ground state.[49] Within the sensitivity of the measurement, there is no detectable long-lived photoproduct. Somewhat slower dynamics are observed in water and ethanol following excitation at 400 nm (Figure 8). No significant long-lived absorption

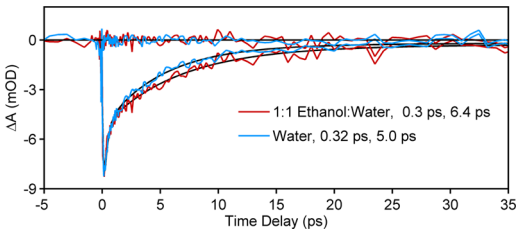

Figure 8. Transient absorption signal at 540 nm following excitation of OHCbl at 400 nm. The traces were fit to a biexponential decay with time constants as indicated with negligible residuals.

change is observed in any of the measurements, setting an upper limit of ca. 1% or less on bond homolysis.

Recent TD-DFT calculations indicate that the excited state potential energy surfaces for OHCbl are distinctly different than those for CNCbl.[24] Several states characterized qualitatively as $n_O + d_{xy} \rightarrow \pi^*$ or $n_O + d_{xy} \rightarrow \sigma^* + d + \pi^*$ fall below the $\pi \rightarrow \pi^*$ states carrying most of the oscillator strength. Bond homolysis may occur via a $n_O + d_{xy} \rightarrow \sigma^* + (d_{xy}$ or $d_{z^2}/d_{xz}) + \pi^*$ channel formed by the S_2 and S_3 states. The S_1 state is a bound $n_O + d_{xy} \rightarrow \pi^*$ MLCT state. Excitation to the optically allowed states is followed by internal conversion to nearly degenerate S_2 and S_3 states followed by branching between the dissociative channel and internal conversion to the S_1 state within a few hundred femtoseconds. Most of the excited state population relaxes to S_1 followed by internal conversion to the ground state on the time scale of a few picoseconds.

3.2. Alkyl Cobalamins

3.2.1. Methyl-, Ethyl-, and Propylcobalamin. The alkyl cobalamins generally exhibit rapid internal conversion to the lowest electronic state followed by cleavage of the C−Co bond with near unit quantum yield on a time scale ranging from ca. 10 to 100 ps.[11−13] Geminate recombination limits the ultimate photolysis yield.[10−12,54,55] MeCbl is an exception with a wavelength dependent quantum yield for bond cleavage.[14] Excitation at 400 nm results in branching between prompt bond cleavage and internal conversion to a low-lying electronic state with a nanosecond lifetime. Excitation at 520 nm eliminates access to the prompt dissociation channel.[14]

The $\alpha\beta$ band of the S_1 state of MeCbl, ethylcobalamin (EtCbl), and propylcobalamin (PrCbl) does not exhibit the blue shift observed for CNCbl.[12,14,20] In these compounds, the S_1 state is

DOI: 10.1021/ar5004016
Acc. Chem. Res. 2015, 48, 860−867

best characterized as a $d/\pi \rightarrow \pi^*$ MLCT state.[21] This assignment is consistent with the solvent dependence of excited state lifetime for MeCbl[20] and with high-level theoretical calculations of the electronic states of MeCbl[25,50] and EtCbl.[50] A more detailed calculation of the S_1 potential energy surface (PES) of MeCbl highlights the potential role of multiple dissociation pathways on the S_1 state.[56] The calculation identifies two regions relevant to the observed photochemistry. The first is characterized as a $(d_{xz}/d_{z^2} + \pi) \rightarrow \pi^*$ transition with MLCT character. The long-lived population in the transient absorption corresponds to the minimum in this region of the PES. The second region is characterized by $(d_{yz} + \pi) \rightarrow \sigma^*(d_{z^2})$ ligand field (LF) character involving a d → d transition of the cobalt. This ligand field state involves substantial elongation and even temporary dissociation of the Co−N_{Im} bond. It is suggested that the LF state plays a significant role in the wavelength dependence of the photolysis of these simple alkylcobalamins.[12,56]

3.2.2. Adenosylcobalamin. At first glance, the photochemistry of AdoCbl is similar to that of the simpler alkylcobalamins. Excitation at 400 or 520 nm results in rapid internal conversion to the lowest electronic state and cleavage of the C−Co bond with near unit quantum yield on a ca. 100 ps time scale.[12,13] A closer look, however, brings to light a significant difference. In contrast to the compounds discussed to this point, the nature of the S_1 state observed in the experiments is dependent on the environment of AdoCbl.[20,54,55] The absorption spectrum of the S_1 state in ethylene glycol resembles that of the non-alkylcobalamins, suggesting that this state exhibits lengthened Co−C and Co−N_{Im} bonds. In water, formation of the equivalent state is followed by internal conversion to a still lower state with an absorption spectrum shifted further to the blue. This blue shift in the absorption spectrum is consistent with an additional lengthening or even temporary dissociation of the Co−N_{Im} bond.[13,20] In the protein environment provided by glutamate mutase, the absorption spectrum of the S_1 state is similar to that observed for MeCbl, EtCbl, and PrCbl.[54,55]

Quantum chemical calculations performed on an AdoCbl model compound shed little light on these observations.[51] The S_1 state calculated using a polarizable continuum model to account for the influence of water is predicted to be a $d/\pi \rightarrow \pi^*$ MLCT state similar to that calculated for MeCbl and EtCbl. It appears that these calculations provide a reasonable model of AdoCbl in glutamate mutase but not in water or ethylene glycol. The nature of the S_1 state in these environments remains uncertain, although the calculated PES of MeCbl may shed some light. The transient absorption data suggest that the LF state is stabilized for AdoCbl in water leading to the blue-shifted S_1 state spectrum.[56] Calculations of AdoCbl currently underway are needed for a more complete understanding.

4. OUTLOOK

The photophysics and photochemistry of ferric porphyrins and cob(III)alamins exhibit both general trends and subtle differences that will prove important for potential applications of these compounds. The strong dipole-allowed optical transitions of the conjugated rings provide a path to efficient electronic excitation. Conversion between electronic states, either of distinct ring $\pi\pi^*$ character or of mixed metal-ring character, dominates the subsequent relaxation of the electronic excitation. A variety of pathways are available resulting in charge transfer, bond cleavage, or ground state recovery. Ultrafast transient absorption spectroscopy with tunable excitation and broadband white light probes spanning large regions from ultraviolet to near-IR wavelengths provides a powerful tool for investigating the dynamics of these systems. The electronic absorption spectra are sensitive to oxidation state, ligation, and spin state of the central metal atoms. When combined with state-of-the-art theoretical simulations and other spectroscopic methods as appropriate, a complete picture of the energy cascade through electronic states emerges. The information from these studies will help to guide development of both porphyrin and cobalamin systems appropriate for applications ranging from energy conversion to drug delivery.

AUTHOR INFORMATION

Corresponding Author

*e-mail: rsension@umich.edu.

Notes

The authors declare no competing financial interest.

Biographies

Aaron S. Rury earned a B.S. in physics from University of Illinois at Urbana−Champaign and an M.S.E. in Electrical Engineering and a Ph.D. in Applied Physics at the University of Michigan. Upon completing a Caltech Postdoctoral Scholarship, he joined the Department of Chemistry at the University of Southern California as a Postdoctoral Scholar studying the ultrafast dynamics of proton-coupled electron transfer. His research interests include ultrafast processes, correlated electron dynamics, and the development of photonics technologies based on molecular building blocks.

Theodore E. Wiley earned his bachelor's degree at The Evergreen State College in 2011. He is currently a Ph.D. candidate working for Professor Roseanne Sension at the University of Michigan. His research focuses on excited state dynamics of molecular rotary motors based on alkene photoisomerization studied by transient absorption spectroscopy.

Roseanne J. Sension received her Ph.D. in 1986 from the University of California, Berkeley. After postdoctoral positions at the University of Oregon and the University of Pennsylvania, she joined the faculty at the University of Michigan in 1992. She is currently a Professor of Chemistry, Physics, and Biophysics at Michigan. Her research interests focus on the fundamental photochemistry and photophysics of light activated molecular devices.

ACKNOWLEDGMENTS

This work was supported by HDTRA1-09-1-0005 and NSF-CHE 1150660. The content of the information does not necessarily reflect the position or the policy of the federal government, and no official endorsement should be inferred. We thank Mr. Brenden Arruda and Dr. Andrew Stickrath for assistance with experimental data shown in Figures 7 and 8.

REFERENCES

(1) Hohmann-Marriott, M. F.; Blankenship, R. E. Evolution of Photosynthesis. *Annu. Rev. Plant Biol.* **2011**, *62*, 515−548.

(2) *The Handbook of Porphyrin Science*; Kadish, K. M., Smith, K. M., Guilard, R., Eds.; World Scientific: Singapore, 2011.

(3) El-Nahass, M. M.; El-Deeb, A. F.; Metwally, H. S.; Hassanien, A. M. Structural and optical properties of iron (III) chloride tetraphenylporphyrin thin films. *Eur. Phys. J.* **2010**, *52*, No. 2010134.

(4) Wende, H.; Bernien, M.; Luo, J.; Sorg, C.; Ponpandian, N.; Kurde, J.; Miguel, J.; Piantek, M.; Xu, X.; Eckhold, P.; Kuch, W.; Baberschke, K.; Panchmatia, P. M.; Sanyal, B.; Oppeneer, P. M.; Eriksson, O. Substrate-induced magnetic ordering and switching of iron porphyrin molecules. *Nat. Mater.* **2007**, *6*, 516−520.

DOI: 10.1021/ar5004016
Acc. Chem. Res. 2015, 48, 860−867

(5) Kar, P.; Sardar, S.; Alarousu, E.; Sun, J. Y.; Seddigi, Z. S.; Ahmed, S. A.; Danish, E. Y.; Mohammed, O. F.; Pal, S. K. Impact of metal ions in porphyrin-based applied materials for visible-light photocatalysis: Key information from ultrafast electronic spectroscopy. *Chem.—Eur. J.* **2014**, *20*, 10475−10483.
(6) Tong, R.; Kohane, D. S. Shedding light on nanomedicine. *Wiley Interdiscip. Rev.: Nanomed. Nanobiotechnol.* **2012**, *4*, 638−662.
(7) Celli, J. P.; Spring, B. Q.; Rizvi, I.; Evans, C. L.; Samkoe, K. S.; Verma, S.; Pogue, B. W.; Hasan, T. Imaging and Photodynamic Therapy: Mechanisms, Monitoring, and Optimization. *Chem. Rev.* **2010**, *110*, 2795−2838.
(8) Banerjee, R.; Ragsdale, S. W. The many faces of vitamin B-12: Catalysis by cobalamin-dependent enzymes. *Annu. Rev. Biochem.* **2003**, *72*, 209−247.
(9) Randaccio, L.; Geremia, S.; Demitri, N.; Wuerges, J. Vitamin B-12: Unique metalorganic compounds and the most complex vitamins. *Molecules* **2010**, *15*, 3228−3259.
(10) Stickrath, A.; Carroll, E. C.; Dai, X.; Harris, D. A.; Rury, A.; Smith, B.; Tang, K.-C.; Wert, J.; Sension, R. J. Solvent-dependent cage dynamics of small nonpolar radicals: Lessons from the photodissociation and geminate recombination of alkylcobalamins. *J. Phys. Chem. A* **2009**, *113*, 8513−8522.
(11) Sension, R. J.; Harris, D. A.; Cole, A. G. Time-resolved spectroscopic studies of B_{12} coenzymes: A comparison of the influence of solvent on the primary photolysis mechanism and geminate recombination of methyl-, ethyl-, n-propyl-, and 5′-deoxyadenosylcobalamin. *J. Phys. Chem. B* **2005**, *109*, 21954−21962.
(12) Cole, A. G.; Yoder, L. M.; Shiang, J. J.; Anderson, N. A.; Walker, L. A., II; Banaszak Holl, M. M.; Sension, R. J. Time-resolved spectroscopic studies of B12 coenzymes: A comparison of the primary photolysis mechanism in methyl-, ethyl-, n-propyl-, and 5′-deoxyadenosylcobalamin. *J. Am. Chem. Soc.* **2002**, *124*, 434−441.
(13) Yoder, L. M.; Cole, A. G.; Walker, L. A., II; Sension, R. J. Time-resolved spectroscopic studies of B12 coenzymes: Influence of solvent on the photolysis of adenosylcobalamin. *J. Phys. Chem. B* **2001**, *105*, 12180−12188.
(14) Shiang, J. J.; Walker, L. A., II; Anderson, N. A.; Cole, A. G.; Sension, R. J. Time-resolved spectroscopic studies of B12 coenzymes: The photolysis of methylcobalamin is wavelength dependent. *J. Phys. Chem. B* **1999**, *103*, 10532−10539.
(15) Shell, T. A.; Shell, J. R.; Rodgers, Z. L.; Lawrence, D. S. Tunable visible and near-IR photoactivation of light-responsive compounds by using fluorophores as light-capturing antennas. *Angew. Chem., Int. Ed.* **2014**, *53*, 875−878.
(16) Rutkowska-Zbik, D.; Mazur, G.; Drzewiecka-Matuszek, A.; Orzel, L.; Stochel, G. Exploring novel modified vitamin B-12 as a drug carrier: Forecast from density functional theory modeling. *J. Phys. Chem. B* **2013**, *117*, 9655−9661.
(17) Shell, T. A.; Lawrence, D. S. A new trick (hydroxyl radical generation) for an old vitamin (B-12). *J. Am. Chem. Soc.* **2011**, *133*, 2148−2150.
(18) Consani, C.; Aubock, G.; Bram, O.; van Mourik, F.; Chergui, M. A cascade through spin states in the ultrafast haem relaxation of metmyoglobin. *J. Chem. Phys.* **2014**, *140*, No. 025103.
(19) Rury, A. S.; Sension, R. J. Broadband ultrafast transient absorption of iron (III) tetraphenylporphyrin chloride in the condensed phase. *Chem. Phys.* **2013**, *422*, 220−228.
(20) Harris, D. A.; Stickrath, A. B.; Carroll, E. C.; Sension, R. J. Influence of environment on the electronic structure of cob(III)alamins: Time-resolved absorption studies of the S1 state spectrum and dynamics. *J. Am. Chem. Soc.* **2007**, *129*, 7578−7585.
(21) Shiang, J. J.; Cole, A. G.; Sension, R. J.; Hang, K.; Weng, Y.; Trommel, J. S.; Marzilli, L. G.; Lian, T. Ultrafast excited-state dynamics in vitamin B12 and related cob(III)alamins. *J. Am. Chem. Soc.* **2006**, *128*, 801−808.
(22) Lodowski, P.; Jaworska, M.; Andruniów, T.; Garabato, B. D.; Kozlowski, P. M. Mechanism of the S1 excited state internal conversion in vitamin B12. *Phys. Chem. Chem. Phys.* **2014**, *16*, 18675−18679.
(23) Kornobis, K.; Kumar, N.; Lodowski, P.; Jaworska, M.; Piecuch, P.; Lutz, J. J.; Wong, B. M.; Kozlowski, P. M. Electronic structure of the S1 state in methylcobalamin: Insight from CASSCF/MC-XQDPT2, EOM-CCSD, and TD-DFT calculations. *J. Comput. Chem.* **2013**, *34*, 987−1004.
(24) Kumar, M.; Kozlowski, P. M. Why hydroxocobalamin is photocatalytically active? *Chem. Phys. Lett.* **2012**, *543*, 133−136.
(25) Solheim, H.; Kornobis, K.; Ruud, K.; Kozlowski, P. M. Electronically excited states of vitamin B-12 and methylcobalamin: Theoretical analysis of absorption, CD, and MCD data. *J. Phys. Chem. B* **2011**, *115*, 737−748.
(26) Lodowski, P.; Jaworska, M.; Kornobis, K.; Andruniow, T.; Kozlowski, P. M. Electronic and structural properties of low-lying excited states of vitamin B-12. *J. Phys. Chem. B* **2011**, *115*, 13304−13319.
(27) Stranius, K.; Iashin, V.; Nikkonen, T.; Muuronen, M.; Helaja, J.; Tkachenko, N. Effect of mutual position of electron donor and acceptor on photoinduced electron transfer in supramolecular chlorophyll-fullerene dyads. *J. Phys. Chem. A* **2014**, *118*, 1420−1429.
(28) Ju, M. G.; Liang, W. Z. Computational insight on the working principles of zinc porphyrin dye-sensitized solar cells. *J. Phys. Chem. C* **2013**, *117*, 14899−14911.
(29) Oberda, K.; Deperasinska, I.; Nizhnik, Y.; Jerzykiewicz, L.; Szemik-Hojniak, A. Photoinduced electron transfer in pentacoordinated complex of zinc tetraphenylporphyrin and isoquinoline N-oxide. Crystal structure, spectroscopy and DFT studies. *Polyhedron* **2011**, *30*, 2391−2399.
(30) Hirao, H. Which DFT functional performs well in the calculation of methylcobalamin? Comparison of the B3LYP and BP86 functionals and evaluation of the impact of empirical dispersion correction. *J. Phys. Chem. A* **2011**, *115*, 9308−9313.
(31) Rajapakse, G. V. N.; Soldatova, A. V.; Rodgers, M. A. J. Photophysical behavior of open-shell, first-row transition metal meso-tetraphenyltetrabenzoporphyrms insights from experimental and theoretical studies. *J. Phys. Chem. B* **2010**, *114*, 14205−14213.
(32) Patra, R.; Bhowmik, S.; Ghosh, S. K.; Rath, S. P. Effects of axial pyridine coordination on a saddle-distorted porphyrin macrocycle: Stabilization of hexa-coordinated high-spin Fe(III) and air-stable low-spin iron(II) porphyrinates. *Dalton Trans.* **2010**, *39*, 5795−5806.
(33) Praneeth, V. K. K.; Paulat, F.; Berto, T. C.; George, S. D.; Nather, C.; Sulok, C. D.; Lehnert, N. Electronic structure of six-coordinate iron(III)-porphyrin NO adducts: The elusive iron(III)-NO(radical) state and its influence on the properties of these complexes. *J. Am. Chem. Soc.* **2008**, *130*, 15288−15303.
(34) Ye, X. O.; Demidov, A.; Rosca, F.; Wang, W.; Kumar, A.; Ionascu, D.; Zhu, L. Y.; Barrick, D.; Wharton, D.; Champion, P. M. Investigations of heme protein absorption line shapes, vibrational relaxation, and resonance Raman scattering on ultrafast time scales. *J. Phys. Chem. A* **2003**, *107*, 8156−8165.
(35) Rury, A. S.; Goodrich, L. E.; Galinato, M. G. I.; Lehnert, N.; Sension, R. J. Ligand recruitment and spin transitions in the solid-state photochemistry of Fe(III)TPPCl. *J. Phys. Chem. A* **2012**, *116*, 8321−8333.
(36) Paulat, F.; Lehnert, N. Detailed assignment of the magnetic circular dichroism and UV-vis spectra of five-coordinate high-spin ferric [Fe(TPP)(Cl)]. *Inorg. Chem.* **2008**, *47*, 4963−4976.
(37) Paulat, F.; Praneeth, V. K. K.; Nather, C.; Lehnert, N. Quantum chemistry-based analysis of the vibrational spectra of five-coordinate metalloporphyrins [M(TPP)Cl]. *Inorg. Chem.* **2006**, *45*, 2835−2856.
(38) Rodriguez, J.; Kirmaier, C.; Holten, D. Optical-properties of metalloporphyrin excited-states. *J. Am. Chem. Soc.* **1989**, *111*, 6500−6506.
(39) Rodriguez, J.; Holten, D. Ultrafast vibrational dynamics of a photoexcited metalloporphyrin. *J. Chem. Phys.* **1989**, *91*, 3525−3531.
(40) Spiro, T. G.; Czernuszewicz, R. S.; Li, X.-Y. Metalloporphyrin structure and dynamics from resonance Raman spectroscopy. *Coord. Chem. Rev.* **1990**, *100*, 541−571.
(41) Burke, J. M.; Kincaid, J. R.; Peters, S.; Gagne, R. R.; Collman, J. P.; Spiro, T. G. Structure-sensitive resonance raman bands of tetraphenyl

DOI: 10.1021/ar5004016
Acc. Chem. Res. 2015, 48, 860−867

and picket fence porphyrin−iron complexes, including an oxy-hemoglobin analog. *J. Am. Chem. Soc.* **1978**, *100*, 6083−6088.
(42) Oshio, H.; Ama, T.; Watanabe, T.; Kincaid, J.; Nakamoto, K. Structure sensitive bands in the vibrational-spectra of metal-complexes of tetraphenylporphine. *Spectrochim. Acta, Part A* **1984**, *40*, 863−870.
(43) Parthasarathi, N.; Hansen, C.; Yamaguchi, S.; Spiro, T. G. Metalloporphyrin core size resonance Raman marker bands revisited - implications for the interpretation of hemoglobin photoproduct Raman frequencies. *J. Am. Chem. Soc.* **1987**, *109*, 3865−3871.
(44) Evans, D. R.; Fackler, N. L. P.; Xie, Z. W.; Rickard, C. E. F.; Boyd, P. D. W.; Reed, C. A. π-Arene/cation structure and bonding. Solvation versus ligand binding in iron(III) tetraphenylporphyrin complexes of benzene, toluene, *p*-xylene, and [60]fullerene. *J. Am. Chem. Soc.* **1999**, *121*, 8466−8474.
(45) Kincaid, J. R.; Proniewicz, L. M.; Bajdor, K.; Bruha, A.; Nakamoto, K. Resonance Raman-spectra of O-2 adducts of cobalt porphyrins - enhancement of solvent and solute bands via resonance vibrational coupling. *J. Am. Chem. Soc.* **1985**, *107*, 6775−6781.
(46) Drennan, C. L.; Huang, S.; Drummond, J. T.; Matthews, R. G.; Ludwig, M. L. How a protein binds B12: A 3.0 Å X-ray structure of B12 domains of methionine synthase. *Science* **1994**, *266*, 1669−1674.
(47) Padovani, D.; Labunska, T.; Palfey, B. A.; Ballou, D. P.; Banerjee, R. Adenosyltransferase tailors and delivers coenzyme B-12. *Nat. Chem. Biol.* **2008**, *4*, 194−196.
(48) Yamanishi, M.; Labunska, T.; Banerjee, R. Mirror "base-off" conformation of coenzyme B12 in human adenosyltransferase and its downstream target, methylmalonyl-CoA mutase. *J. Am. Chem. Soc.* **2005**, *127*, 526−527.
(49) Jones, A. R.; Russell, H. J.; Greetham, G. M.; Towrie, M.; Hay, S.; Scrutton, N. S. Ultrafast infrared spectral fingerprints of vitamin B-12 and related cobalamins. *J. Phys. Chem. A* **2012**, *116*, 5586−5594.
(50) Lodowski, P.; Jaworska, M.; Andruniow, T.; Kumar, M.; Kozlowski, P. M. Photodissociation of Co-C bond in methyl- and ethylcobalamin: An insight from TD-DFT calculations. *J. Phys. Chem. B* **2009**, *113*, 6898−6909.
(51) Andruniow, T.; Jaworska, M.; Lodowski, P.; Zgierski, M. Z.; Dreos, R.; Randaccio, L.; Kozlowski, P. M. Time-dependent density functional theory study of cobalt corrinoids: Electronically excited states of coenzyme B-12. *J. Chem. Phys.* **2009**, *131*, No. 105105.
(52) Andruniów, T.; Jaworska, M.; Lodowski, P.; Zgierski, M. Z.; Dreos, R.; Randaccio, L.; Kozlowski, P. M. Time-dependent density functional theory study of cobalt corrinoids: Electronically excited states of methylcobalamin. *J. Chem. Phys.* **2008**, *129*, No. 085101.
(53) Kornobis, K.; Kumar, N.; Wong, B. M.; Lodowski, P.; Jaworska, M.; Andruniow, T.; Ruud, K.; Kozlowski, P. M. Electronically excited states of vitamin B-12: Benchmark calculations including time-dependent density functional theory and correlated ab initio methods. *J. Phys. Chem. A* **2011**, *115*, 1280−1292.
(54) Sension, R. J.; Harris, D. A.; Stickrath, A.; Cole, A. G.; Fox, C. C.; Marsh, E. N. G. Time-resolved measurements of the photolysis and recombination of adenosylcobalamin bound to glutamate mutase. *J. Phys. Chem. B* **2005**, *109*, 18146−18152.
(55) Sension, R. J.; Cole, A. G.; Harris, A. D.; Fox, C. C.; Woodbury, N. W.; Lin, S.; Marsh, E. N. G. Photolysis and recombination of adenosylcobalamin bound to glutamate mutase. *J. Am. Chem. Soc.* **2004**, *126*, 1598−1599.
(56) Lodowski, P.; Jaworska, M.; Andruniow, T.; Garabato, B. D.; Kozlowski, P. M. Mechanism of Co−C bond photolysis in the base-on form of methylcobalamin. *J. Phys. Chem. A* **2014**, *118*, 11718−11734.

DOI: 10.1021/ar5004016
Acc. Chem. Res. 2015, 48, 860−867